PHYSICAL REVIEW B VOLUME 23, NUMBER 8 15 APRIL 1981

Theory of electron-phason scattering and the low-temperature resistivity of potassium

Marilyn F. Bishop
Department of Physics and Atmospheric Science, Drexel University, Philadelphia, Pennsylvania 19104

A. W. Overhauser
Department of Physics, Purdue University, West Lafayette, Indiana 47907

(Received 24 October 1980)

Scattering of electrons by phasons, the collective excitations of an incommensurate charge-density wave (CDW), is presented as a new mechanism in the low-temperature resistivity of potassium. It is shown to provide an explanation for recent precision measurements in potassium between 0.38 and 1.3 K, where conventional mechanisms, such as electron-electron scattering, fail. With this theory, it is possible to explain the shape of the measured resistivity curves, the magnitude of the temperature-dependent part of the resistivity, and the sample dependence. The sample dependence is explained since the measured electron-phason resistivity, which is much larger along the CDW wave vector $\vec{Q}$ than perpendicular to it, depends on the $\vec{Q}$-domain structure of a particular sample. Fitting this theory to these experiments yields the value for the phason temperature $\Theta_\phi = 3.25$ K and an approximate range of the anisotropy of the phason spectrum, $7.7 \lesssim (1/\eta) \lesssim 9.7$. Further resistivity measurements at ultralow temperatures are needed to test the hypothesis of electron-phason scattering, and, if this mechanism continues to show promise, to provide more accurate estimates for the phason parameters.

I. INTRODUCTION

Results of recent measurements of the low-temperature electrical resistivity of several simple metals have rejuvenated interest in the basic scattering mechanisms of electrons. One of the motivations for performing these experiments was the desire to find evidence for electron-electron scattering, which was predicted to produce a T^2 term in the resistivity, independent of the residual resistivity ρ_0. Therefore, reports of approximate T^2 variations of electrical resistivity below 2 K in potassium,[1-4] aluminum,[4,5] silver,[6] and copper[7] have sparked considerable excitement. However, the interpretation of these data in terms of electron-electron scattering is, in some cases, open to question. Basic discrepancies exist, for example in potassium, between the experiments and the theory in terms of electron-electron scattering.

Only in aluminum has it been shown that the T^2 term is independent of ρ_0.[5] In fact, in K, the temperature-dependent part of the resistivity increases rapidly with increasing ρ_0. In addition, in K, a T^2 behavior is actually inconsistent with the data. A pure power-law fit[2] produces $T^{1.5}$, but the dependence is probably more complicated. No conventional mechanism can reconcile the observed behavior. For this reason, we suggest that a new scattering mechanism must be invoked,[8] namely, the scattering of electrons from phasons,[9] excitations associated with phase fluctuations of a charge-density wave (CDW).

The objectives of this paper are to show that all conventional mechanisms fail to explain existing data in K and to demonstrate that the theory of electron-phason scattering can explain both the shape and magnitude of the resistivity anomaly. Previously, in Ref. 8, we presented a limiting case of this theory and illustrated its ability to fit the shape of the measured curves. The paper is organized as follows. In Sec. II, we analyze existing experiments in potassium and discuss conventional resistivity mechanisms. In Sec. III, we review the properties of charge-density waves and phasons and of the electron-phason interaction. In addition, we calculate the resulting transition matrix elements. We present in Sec. IV a derivation of the expressions used in calculations of the electron-phason resistivity and in Sec. V the results of numerical evaluations of these expressions. Finally, in Sec. VI, we state the conclusions.

II. ANALYSIS OF EXPERIMENTS

In order to understand the recent measurements of the low-temperature resistivity of potassium, let us first consider the conventional theoretical ideas about the contributions to the resistivity $\rho(T)$ of a simple metal at low temperatures,[10]

$$\rho(T) = \rho_0 + AT^5 + BT^p \exp(-\hbar\omega_0/k_B T) + CT^2 \ , \quad (2.1)$$

where ρ_0 is the residual resistivity, a temperature-independent part of the resistivity due to scattering of electrons from impurities and other imperfections in the crystal. The term AT^5 is the low-temperature limiting behavior of the resistivity resulting from normal electron-phonon scat-

tering. If phonon-drag effects are important, i.e., if the phonons drift with the electrons, then the magnitude of this term can be greatly reduced. Electron-phonon umklapp scattering, which is unaffected by phonon drag, contributes a term of the form $BT^p \exp(-\hbar\omega_0/k_BT)$, where ω_0 is the frequency of the phonon with the minimum wave vector that allows the electrons to scatter via an umklapp process. Electron-electron scattering adds a term CT^2 at all temperatures. The assumption that each of these contributions can be added independently is known as Matthiessen's rule.

The determination of the relative importance of each of the above mechanisms has been the object of considerable experimental study. The first of the temperature-dependent terms in Eq. (2.1) to be verified was the exponential decay of the electron-phonon umklapp scattering with decreasing temperature below 4 K.[11] Later, theoretical predictions[12-14] of the possibility of detecting the effects of phonon drag at temperatures below 2 K encouraged further low-temperature work. An additional incentive was that if phonon drag diminished the T^5 of normal electron-phonon processes, the only significant remaining temperature-dependent contribution to the resistivity below 2 K might be that of the CT^2 term in Eq. (2.1) due to electron-electron scattering.[15]

Van Kempen *et al.*[1] measured the temperature-dependent resistivity of potassium between 1.1 and 4.2 K and found evidence for the presence of phonon drag. The magnitude of the resistivity dipped well below the predicted magnitude for the AT^5 that would be present in the absence of phonon drag. Below 2 K, an anomalous sample-dependent component of the resistivity appeared. Since the variation of this new term was consistent with T^2, van Kempen *et al.* suggested that this might be due to electron-electron scattering. Unfortunately, this contribution to the resistivity was sample dependent, in contradiction to conventional theories of electron-electron scattering.[15] In addition, the presence of the exponential tail due to electron-phonon umklapp scattering causes some difficulty in determining the exact temperature dependence of this newly observed feature in the resistivity. Ideally, the umklapp scattering portion of the resistivity should be subtracted from the data before analyzing any new contribution. Unfortunately, difficulties arise because of a lack of knowledge of the exact form of this function below 2 K. While van Kempen *et al.* were able to fit their data well with the exponential term given in Eq. (2.1) with $p = 1$ and $\Theta = \hbar\omega_0/k_B = 19.9$, Kaveh, Leavens, and Wiser[16] point out that the validity of extending this form below 2 K is questionable. One may avoid this difficulty by considering only data below which electron-phonon umklapp scattering is negligible compared with the new component of the low-temperature resistivity, i.e., below about 1.3 K. Clearly, then, the remaining temperature range between 1.1 and 1.3 K is too narrow to confirm or deny a T^2 dependence.

This uncertainty prompted Rowlands, Duvvury, and Woods[2] to extend the low-temperature resistivity measurements of potassium down to 0.4 K. Between 4 and 2 K, their data agreed with the previous results. However, they found that, with the extended range of temperatures, the data below 1.3 K were inconsistent with a T^2 dependence, and that the best pure power law that would fit the data was actually $T^{1.5}$. On the other hand, this data need not be fitted to a pure power law. In fact, in a previous paper,[8] we showed that the shape of the curve, as well as its sample dependence, could be explained by the scattering of electrons from phasons, the phase fluctuations of a charge-density wave, and this theory yielded Bloch-Grüneisen functions rather than a pure power law.

The sample dependence of the new component in the temperature-dependent resistivity impelled Levy *et al.*[3] to study this aspect further. They measured a variety of samples, with $\rho(T) - \rho_0$ ranging from 8×10^{-14} to 4.2×10^{-13} Ω cm at 1.2 K, where ρ_0 was guessed in order to obtain a T^2 fit. This range of magnitudes was comparable to what was seen in other measurements. Although they ascribed a T^2 dependence to the anomalous resistivity, their measurements, which did not extend below 1.1 K, could not determine that behavior. They suggested that the data could be explained by a theory of Kaveh and Wiser,[17] in which normal electron-electron processes contribute to the resistivity as the result of anisotropic electron-dislocation scattering, in a breakdown of Matthiessen's rule.

Essentially, the idea is that when electrons scatter from the anisotropic dislocation lines, the steady-state distribution function in the presence of an electric field is distorted in shape from that of the equilibrium distribution function, i.e., a "dimple" forms in the direction of the field. Normal electron-electron scattering can be thought of as a diffusion of electrons on the Fermi surface, and this diffusion "heals" the "dimple" in such a way as to restore the shape of the equilibrium distribution function. In this way, a resistivity arises that is dependent on the density of dislocations and on the normal electron-electron scattering, which varies as T^2.

In order to explain their data in terms of this theory, Levy *et al.*[3] imposed two major assumptions. First, they assumed that the anomalous temperature-dependent resistivity varies as T^2,

in contradiction to the measurements of Rowlands *et al.*[2] Second, they supposed that all their samples had a resistivity, $\rho_{0D} = 0.4$ nΩ cm, due to electron-dislocation scattering, independent of impurity concentration or annealing time. (Some samples annealed for more than a month.) No direct measurement was done of the dislocation density or impurity concentration.

The validity of assuming such a large value for ρ_{0D} is questionable. It is known that ρ_{0D} is related, in K, to the dislocation density n_D by[18,19]

$$\rho_{0D} \simeq 4\times10^{-19} n_D, \tag{2.2}$$

where ρ_{0D} is in Ω cm and n_D is in cm^{-2}. This relation was extracted from measurements of the resistivity as a function of strain and of strain as a function of applied stress.[20] In obtaining Eq. (2.2), the assumption was made that the relation for dislocation density as a function of applied stress, which was determined in the noble metals by electron microscopy and etch pit experiments, may be applied to alkali metals. Thus the value chosen by Levy *et al.* for ρ_{0D} corresponds to a dislocation density of 10^9 cm^{-2}.

Kaveh and Wiser extended the above analysis of low-temperature resistivity measurements in K in terms of their theory by including the data of van Kempen *et al.*[1] and of Rowlands *et al.*,[2] in addition to that of Levy *et al.*[3] They assumed resistivities due to electron-dislocation scattering of $\rho_{0D} \sim 0.53$–1.8 nΩ cm for van Kempen *et al.* and $\rho_{0D} \sim 1.5$–4.8 nΩ cm for Rowlands *et al.*, corresponding to dislocation densities of $n_D \sim 1.3\times10^9 - 4.5\times10^9$ cm^{-2} and $n_D \sim 1.8\times10^9 - 1.2\times10^{10}$ cm^{-2}, respectively.

The magnitudes of dislocation densities presumed to exist in unstressed samples of K by Levy *et al.*[3] and Kaveh and Wiser[17] is unreasonably large compared with values obtained from direct measurements. In neutron diffraction experiments of potassium by Overhauser[9] and by Stetter *et al.*,[21] it was determined from the rocking curve that the angular mosaic spread was about 0.1 degrees and from primary extinction measurements that the mosaic block was of the order of 1 mm. This corresponds to a dislocation density of less than 10^6 cm^{-2}. In addition, it was found that dislocations produced by thermal stress anneal out in less than an hour.[9] These numbers are then at least 3 orders of magnitude smaller than those assumed by Levy *et al.*[3] and by Kaveh and Wiser[17] in order to explain the data in terms of electron-electron scattering enhanced by electron-dislocation scattering.

In fact, high dislocation densities imply that samples are strained by a significant amount. As given in Eq. (2.2), the dislocation density n_D of a sample is related to the resistivity caused by those dislocations. Basinski *et al.*[20] found that large resistivities due to dislocations ρ_{0D} or high dislocation densities n_D were actually difficult to achieve. They found that, for small strains, the resistivity increases ~1.3% per percent strain, which was also found by Jones.[22] However, large external stresses were required to produce even small strains. For instance, for the dislocation resistivity ρ_{0D} suggested by Levy *et al.*,[3] $\rho_{0D} = 0.4$ nΩ cm, the strain required would be about 3.5%, which is attained when the sample is under an external stress of 0.75 kg/mm^2. The largest strain that was achieved in any sample before the wire broke was about 16%, under a stress of nearly 1 kg/mm^2, which corresponds to a dislocation density of $n_D \sim 7\times10^9$ cm^{-2}. This is considerably smaller than the largest dislocation density assumed by Kaveh and Wiser,[17] $\rho_{0D} = 1.2\times10^{10}$ cm^{-2}, in presumably stress-free samples.

Further difficulties with assuming arrays of oriented dislocations to be responsible for anomalous results in potassium come from other experiments. For example, the resistivity tensor of a single crystal of potassium has been measured to be a cigar-shaped ellipsoid with an anisotropy of 4 or 5 to 1.[23,24] If oriented arrays of dislocations were responsible for this effect, the resistivity tensor would have to be a pancake-shaped ellipsoid, since dislocation lines can be thought of as cylindrically-shaped scattering centers that only scatter electrons that travel perpendicular to the axis of the cylinder.

We now turn our attention to a closer examination of the temperature dependence of the new component in the resistivity. We point out that the best way to analyze the temperature dependence is to employ a procedure that does not depend on the subtraction of the residual resistivity ρ_0 from the data. For instance, a logarithmic plot of the data requires this subtraction, and the extracted temperature dependence of the data can depend on the guess one makes for the magnitude of the residual resistivity. Rowlands *et al.*[2] avoided this difficulty by plotting the total resistivity versus T^n and choosing the value of n that gave a straight line. Here, we plot the data on a linear-linear plot to avoid the problem. In Fig. 1, we plot with circles the data of sample K2c of Rowlands *et al.*,[2] where the zero of resistivity was set at the lowest data point. The two points above 1.3 K are displayed to illustrate the residual contribution of electron-phonon umklapp scattering to these points. The dashed arrows indicate the magnitudes one would subtract from the data if the exponential term in Eq. (2.1) were used with the parameters of van Kempen *et al.*[1] for fitting the data in the region

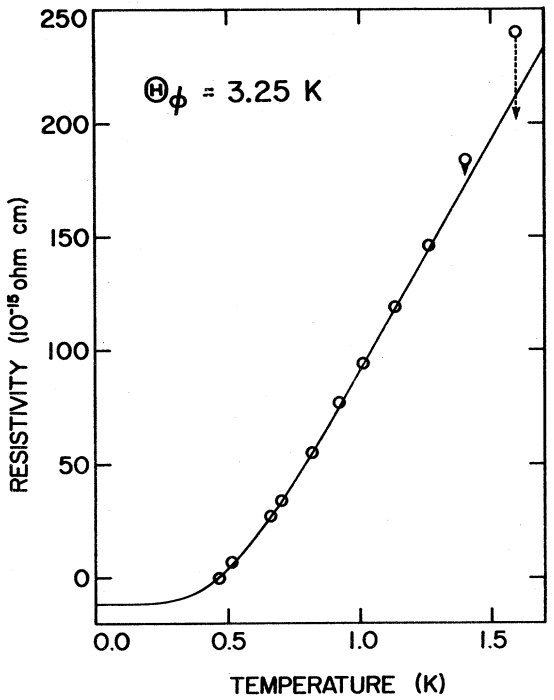

FIG. 1. Plot of resistivity versus temperature for the data of sample K2c of Rowlands, Duvvury, and Woods (Ref. 1) indicated by circles. The curve and arrows are described in the text.

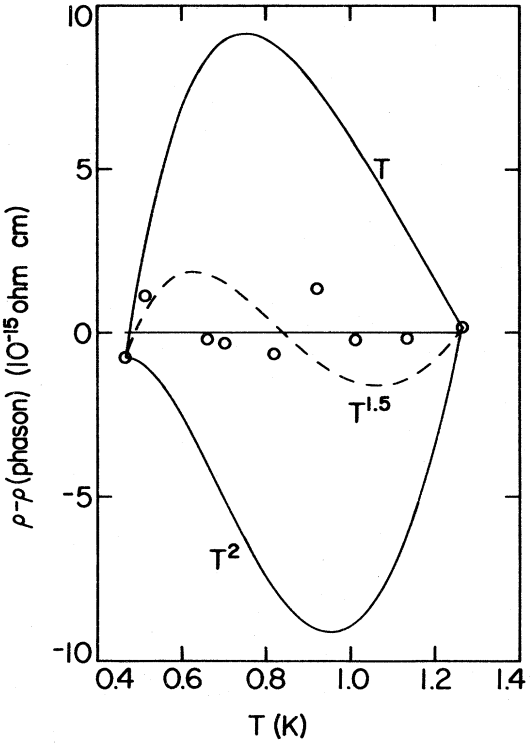

FIG. 2. Plot of resistivity subtracted from ρ(phason), the smooth curve through the data in Fig. 1. The data of Fig. 1 are shown as circles scattered about the horizontal line ρ(phason). Curves labeled T, $T^{1.5}$, and T^2 are the corresponding pure power laws that pass through the first and last data points below 1.3 K.

between 2 and 4 K. A solid curve has been drawn through all but the two highest data points. We call this curve ρ(phason), since it is actually the result of the theory of electron-phason scattering, which is presented in this paper.

There is no evidence of a T^5 dependence, which is consistent with the existence of phonon drag. A T^2 curve is also the wrong shape to fit the data. This is more obvious in Fig. 2, where we show directly the difference between a T^2 curve and a smooth curve through the data. The horizontal line is ρ(phason), the smooth curve through the data in Fig. 1, which we use as a reference, and we plot $\rho-\rho$(phason), where ρ is given either by the data (circles) or by the power laws in T, $T^{1.5}$ and T^2, that pass through the first and last data points below 1.3 K. Clearly the T^2 curve is the wrong shape to describe the data. In fact, that fit is as poor as a straight line through the data (the curve labeled T). If one requires the best-fit pure power law, one obtains $T^{1.5}$, as was first illustrated by Rowlands *et al.*[2] The estimated error in the data[2] was $\pm 10^{-15}$ Ω cm, which is about the same as the scatter of the data about the horizontal line. The temperature dependence of this data thus rules out electron-electron scattering, at least as the principal mechanism, as an explanation of the data. As we will show in the following sections, the scattering of electrons from phasons, the collective excitations corresponding to phase modulation of a charge-density wave, can explain the shape,[8] as well as the magnitude, of this new anomalous component in the low-temperature resistivity of potassium.

III. PHASONS AND THE ELECTRON-PHASON INTERACTION

A charge-density wave (CDW) is characterized by a static sinusoidal modulation of the electronic charge density,

$$\rho(\vec{r}) = \rho_0[1 + p\cos(\vec{Q}\cdot\vec{r} + \phi)], \tag{3.1}$$

where ρ_0 is the average density, p is the fractional modulation, and ϕ is the phase. The magnitude of the CDW wave vector $\vec{Q}$ is approximately the diameter of the Fermi surface. It has been shown that, within the deformable jellium model, such a structure lowers the exchange and correlation energies with respect to those of the state characterized by a uniform charge density.[25] However, large static electric fields will develop in the metal unless the lattice undergoes a compensating distortion in order to ensure macroscopic charge

neutrality,

$$\vec{u}(\vec{L}) = \vec{A}\sin(\vec{Q}\cdot\vec{L}+\phi)\ , \tag{3.2}$$

where $\vec{u}(\vec{L})$ is the displacement of the ion from its original site $\vec{L}$, and $\vec{A}$ is the maximum amplitude of that displacement. Theoretically, it has been shown that, in the alkali metals, the lattice provides almost a complete screening of the electric fields produced by the electronic density $\rho(\vec{r})$.[26]

Considerable experimental evidence supports the existence of a CDW ground state in the alkali metals, especially in potassium. The experimental situation in potassium was reviewed recently.[27] Even more recently, the observation of anomalies in the de Haas–van Alphen effect under pressure[28] and of open orbits[29] by the induced torque method have further strengthened the case of the CDW ground state in potassium. Although the predicted CDW diffraction satellites[9,30] have not yet been observed,[31] neutron diffraction experiments have not been performed with sufficient sensitivity to detect the estimated intensities.[32]

In the alkali metals, the CDW is incommensurate, since the CDW wave vector $\vec{Q}$, which spans the Fermi surface, is not related to any reciprocal-lattice vector by a small integer. For this reason, for very pure samples, the energy of the system does not depend on the value of the phase ϕ. This invariance of the energy leads to low-frequency collective excitations called phasons whose frequency spectrum goes to zero at the point $\vec{Q}$ in $\vec{k}$ space. The phase $\phi(\vec{r},t)$ of the electronic charge density is modulated slowly in space and time, and the phase $\phi(\vec{L},t)$ of the lattice follows, so as to screen out the electron density,

$$\phi(\vec{L},t) = \sum_{\vec{q}} \phi_{\vec{q}}\sin(\vec{q}\cdot\vec{L}-\omega_{\vec{q}}t)\ , \tag{3.3}$$

where $\vec{q}$ and $\omega_{\vec{q}}$ are the wave vector and frequency of the phason, and $\phi_{\vec{q}}$ is its amplitude. Thus a phason is actually a normal mode of the lattice whose frequency vanishes at the point $\vec{Q}$ and varies linearly with $\vec{q}$ away from that point.

Although we are concerned in this paper with the influence of phasons on the electrical resistivity, it is interesting to note that these low-frequency excitations can also affect a number of other physical properties. For example, they can produce an anomaly in the low-temperature heat capacity,[33] an effect that was first observed in $LaGe_2$, a three-dimensional system, by Sawada and Satoh.[34] There is even evidence supporting such an anomaly in rubidium, one of the alkali metals.[35,36] Since extensive theoretical studies have been done investigating the general properties of phasons,[9,26,37,38] we will confine our attention here to those aspects that are required in the calculation of the electron-phason resistivity, referring to earlier work for details.

A phason is a coherent linear combination of two "old" phonons, i.e., phonons of the undistorted lattice, of wave vectors $\vec{q}+\vec{Q}$ and $\vec{q}-\vec{Q}$.[9] The orthogonal linear combination of these same two "old" phonons is an amplitude mode,[39] a collective oscillation of the amplitude $\vec{A}$ in Eq. (3.2), which occurs at high frequency. The situation is illustrated schematically in Fig. 3. Away from the points $\vec{Q}$ and $-\vec{Q}$, the phason and amplitude modes merge quickly into the phonon spectrum, so that these new excitations exist only in a very small volume of phase space. For simplicity, we will assume that at some frequency cutoff ω_ϕ, the phasons transform into phonons, and for the purposes of this paper we will neglect the contributions of the phonons and amplitude modes in the calculation of the resistivity. q_ϕ is the corresponding wave-vector cutoff along $\vec{Q}$. We should comment that Fig. 3 has only an approximate meaning, since, in the presence of an incommensurate CDW, the system no longer has translational symmetry along $\vec{Q}$. (Actually, $\vec{Q}$ is longer than half the reciprocal-lattice vector along it.)

As illustrated in Fig. 4, this phason spectrum is expected to be highly anisotropic, such that

$$\omega_{\vec{q}} = (c_\parallel^2 q_\parallel^2 + c_\perp^2 q_\perp^2)^{1/2} = c_\parallel^2(q_\parallel^2+\eta^2 q_\perp^2)^{1/2}\ , \tag{3.4a}$$

where

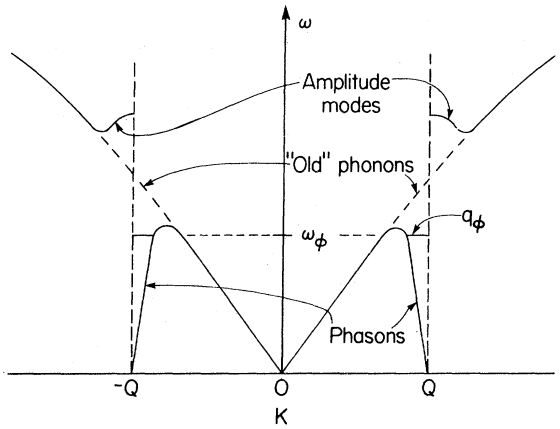

FIG. 3. Schematic illustration of the vibrational modes in a metal having a CDW structure. The frequency of the phason branch goes to zero at $\pm\vec{Q}$. A phason is a linear superposition of two "old" phonons, and the amplitude modes are the orthogonal linear combination. Phason and amplitude modes quickly merge into the new phonon spectrum, as indicated. ω_ϕ and q_ϕ are the frequency and wave-vector cutoffs for the phason that are used in this paper.

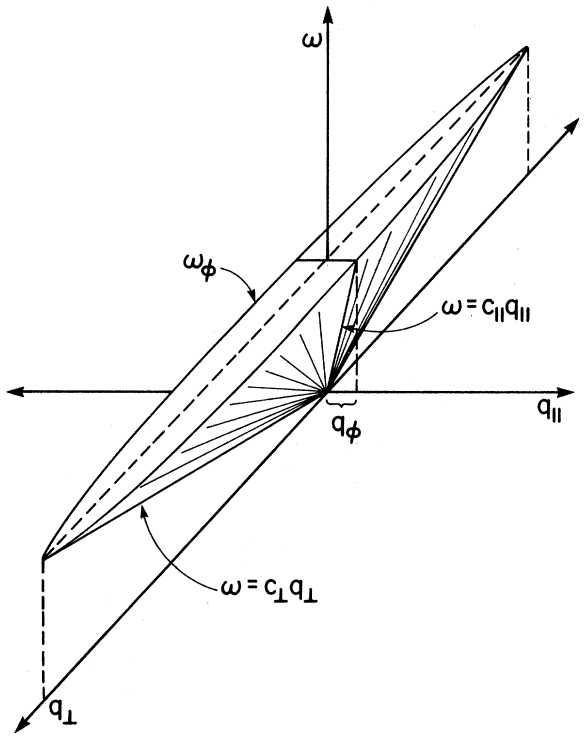

FIG. 4. Anisotropic cone of the phason spectrum, showing the longitudinal and transverse phason velocities $c_{\|}$ and $c_\perp$. ω_ϕ is the frequency cutoff of the phason spectrum and q_ϕ is the wave-vector cutoff along Q.

$$\eta = c_\perp / c_{\|} \ , \tag{3.4b}$$

and where $q_{\|}$ and $q_\perp$ are the components of $\vec{q}$ parallel and perpendicular to the CDW wave vector $\vec{Q}$. Correspondingly, $c_{\|}$ and $c_\perp$ are the phason velocities parallel and perpendicular to $\vec{Q}$, or the longitudinal and transverse phason velocities. A characteristic phason temperature Θ_ϕ can now be identified with the frequency and wave vector cutoffs ω_ϕ and q_ϕ as

$$\Theta_\phi \equiv \hbar \omega_\phi / k_B = \hbar c_{\|} q_\phi / k_B \ . \tag{3.5}$$

This phason temperature can now be determined by the shape of the measured resistivity curve. The value of Θ_ϕ determined from the resistivity will not necessarily be the same as that relevant for the specific heat, since the two measurements probe different properties of the phasons. In the calculation of the specific heat, one must include contributions from all modes (phasons, amplitude modes, phonons). The resistivity, however, depends not only on the modes themselves but on the interaction of electrons with them.

For small $\vec{q}$, the longitudinal phason represents a lengthening and shortening of $\vec{Q}$, while the transverse phason represents a rotation of $\vec{Q}$ about its static value. In the alkali metals, the magnitude of $\vec{Q}$ is related to the same many-electron effects of exchange and correlation that initially gave rise to the CDW instability. The direction of $\vec{Q}$, on the other hand, depends only on the elastic anisotropy of potassium,[30] since the many-electron effects are essentially isotropic. In fact, a calculation of the transverse phason velocity based on this idea has recently been performed[26] and it was found that $c_\perp$ is of the order of the acoustic phonon velocities. The magnitude of the longitudinal velocity $c_{\|}$ is not known, but it is expected to be much larger than the transverse velocity $c_\perp$, since it depends on many-electron interactions. Therefore, η will be much less than unity. In Sec. V, we will show that the low-temperature resistivity measurements limit the acceptable range of values for η. Although the transverse phason spectrum is also anisotropic, we use here the average transverse phason velocity for $c_\perp$.

Since a phason is a harmonic oscillator, its amplitude $\phi_{\vec{q}}$ in Eq. (3.3) can be related to its frequency $\omega_{\vec{q}}$. In order to determine that relation, we follow a procedure similar to that for phonons. We first write $\phi(\vec{L}, t)$ of Eq. (3.3) in the Heisenberg picture in terms of the creation and annihilation operators $a_{\vec{q}}^*$ and $a_{\vec{q}}$ of the harmonic oscillator,

$$\phi(\vec{L}) = \sum_{\vec{q}} \frac{\phi_{\vec{q}}}{2i} \left(a_{\vec{q}} e^{i\vec{q}\cdot\vec{L}} - a_{\vec{q}}^* e^{-i\vec{q}\cdot\vec{L}} \right) . \tag{3.6}$$

For small ϕ, we may rewrite $\vec{u}(\vec{L})$ from Eq. (3.2) as

$$\vec{u}(\vec{L}) = \vec{A} [\sin\vec{Q}\cdot\vec{L} + \phi(\vec{L}) \cos\vec{Q}\cdot\vec{L}] . \tag{3.7}$$

The kinetic energy,

$$T = \tfrac{1}{2} M \sum_{\vec{L}} \left(\frac{d\vec{u}(\vec{L})}{dt} \right)^2 , \tag{3.8}$$

can be written in terms of $\phi(\vec{L})$ if we recognize that $i\hbar(d\vec{u}/dt) = [\vec{u}, \mathcal{H}]$, where $\mathcal{H} = \hbar\omega_{\vec{q}} (a_{\vec{q}}^* a_{\vec{q}} + \frac{1}{2})$. Thus, we have

$$\frac{d\vec{u}(\vec{L})}{dt} = -\vec{A} \cos(\vec{Q}\cdot\vec{L}) \times \sum_{\vec{q}} \frac{\omega_{\vec{q}}}{2} \phi_{\vec{q}} (a_{\vec{q}} e^{i\vec{q}\cdot\vec{L}} + a_{\vec{q}}^* e^{-i\vec{q}\cdot\vec{L}}) , \tag{3.9}$$

and

$$T = \tfrac{1}{4} \rho_m A^2 \sum_{\vec{q}} \frac{\phi_{\vec{q}}^2 \omega_{\vec{q}}^2}{4} (a_{\vec{q}} a_{\vec{q}}^* + a_{\vec{q}}^* a_{\vec{q}}) , \tag{3.10}$$

where ρ_m is the mass density of the crystal, and the volume of a unit cell is set equal to unity. In obtaining this result, Eq. (3.10), we have written $\cos^2(\vec{Q}\cdot\vec{L}) = \frac{1}{2} + \frac{1}{2}\cos(2\vec{Q}\cdot\vec{L})$. The second term

yields zero, since we average over the long wavelength $\vec{q}$ of the phason.

For a harmonic oscillator, $T=\frac{1}{2}W$, where W is the total energy given by

$$W=\hbar\omega_{\vec{q}}(a_{\vec{q}}^{*}a_{\vec{q}}+\tfrac{1}{2})=\tfrac{1}{2}\hbar\omega_{\vec{q}}(a_{\vec{q}}^{*}a_{\vec{q}}+a_{\vec{q}}a_{\vec{q}}^{*}). \tag{3.11}$$

We thus obtain the phason amplitude in terms of $\omega_{\vec{q}}$,

$$\phi_{\vec{q}}=\frac{2}{A}\left(\frac{\hbar}{\rho_m\omega_{\vec{q}}}\right)^{1/2}. \tag{3.12}$$

The property of phasons of most interest in calculating their effect on the low-temperature resistivity is the form of the electron-phason interaction. This may be written formally as

$$V_{e\phi}=G\cos(\vec{Q}\cdot\vec{r}+\phi)-G\cos(\vec{Q}\cdot\vec{r}), \tag{3.13}$$

where $G\cos(\vec{Q}\cdot\vec{r})$ is the static self-consistent one-electron potential of the CDW and $G\cos(\vec{Q}\cdot\vec{r}+\phi)$ is the corresponding potential in the presence of weak phase modulation. For small ϕ, we may rewrite this as

$$V_{e\phi}=-G\phi(\vec{r})\sin\vec{Q}\cdot\vec{r}$$
$$=\frac{G}{4}\sum_{\vec{q}}\phi_{\vec{q}}(a_{\vec{q}}-a_{-\vec{q}}^{*})(e^{i(\vec{q}+\vec{Q})\cdot\vec{r}}-e^{i(\vec{q}-\vec{Q})\cdot\vec{r}}), \tag{3.14}$$

where $\phi(\vec{r})$ is the continuum analog of $\varphi(\vec{L})$ in Eq. (3.6). Note that the wave vector that appears in this expression is not the small wave vector $\vec{q}$ (long wavelength) but the large wave vector $\vec{q}\pm\vec{Q}$ (short wavelength).

In calculating the electron-phason resistivity, we will employ this interaction $V_{e\phi}$ in Eq. (3.14) through the "golden rule" transition rate of an electron scattering from a state labeled $\vec{k}$ to a state labeled $\vec{k}'$:

$$W_{\vec{k}\to\vec{k}'}=\frac{2\pi}{\hbar}|M_{\vec{k},\vec{k}'}|^2\delta(\mathcal{E}_{\vec{k}}^{\mathrm{tot}}-\mathcal{E}_{\vec{k}'}^{\mathrm{tot}})f_{\vec{k}}(1-f_{\vec{k}'}), \tag{3.15}$$

where $\mathcal{E}_{\vec{k}}^{\mathrm{tot}}$ is the total energy of the initial state (including phasons) and $\mathcal{E}_{\vec{k}'}^{\mathrm{tot}}$ is the total energy of the final state. $f_{\vec{k}}$ is the electron distribution function. Here, the scattering matrix element is

$$M_{\vec{k},\vec{k}'}=\langle\Psi_{\vec{k}'},n_{\vec{q}_1},n_{\vec{q}_2},\ldots|V_{e\phi}|\Psi_{\vec{k}},n_{\vec{q}_1},n_{\vec{q}_2},\ldots\rangle, \tag{3.16}$$

where $n_{\vec{q}_1}$ is the number of phasons of wave vector $\vec{q}_1$, $n_{\vec{q}_2}$ is the number of phasons of wave vector $\vec{q}_2$, etc., and $\Psi_{\vec{k}}$ and $\Psi_{\vec{k}'}$ are wave functions corresponding to solutions of the one-electron Schrödinger equation in the presence of a static CDW,

$$\left(\frac{p^2}{2m}+G\cos\vec{Q}\cdot\vec{r}\right)\Psi_{\vec{k}}(\vec{r})=E_{\vec{k}}\Psi_{\vec{k}}(\vec{r}). \tag{3.17}$$

The potential $G\cos\vec{Q}\cdot\vec{r}$ deforms both the wave functions and the energy spectrum by mixing the plane wave state $\vec{k}$ with the plane wave state $\vec{k}\pm\vec{Q}$ and produces the modulated electron density given in Eq. (3.1). This in turn produces energy gaps of magnitude G at $\vec{k}=\pm\vec{Q}/2$ and distorts the spherical Fermi surface in the same region. In addition, the scattering of electrons by phasons is the most intense in this region. Therefore, for simplicity, we translate our coordinate system in $\vec{k}$ space by $\vec{Q}/2$, so that our new $\vec{k}$ is measured with respect to the point $\vec{Q}/2$.

For small G, the plane wave state $\vec{k}+\frac{1}{2}\vec{Q}$ and $\vec{k}-\frac{1}{2}\vec{Q}$ in the new coordinate system are nearly degenerate. We therefore treat the coupling between these two states exactly by solving the following secular equation, which is written in the basis of these two plane waves:

$$\begin{pmatrix}\left(\frac{\hbar^2}{2m}(\vec{k}+\frac{1}{2}\vec{Q})^2-E_{\vec{k}}\right) & \frac{1}{2}G\\ \frac{1}{2}G & \left(\frac{\hbar^2}{2m}(\vec{k}-\frac{1}{2}\vec{Q})^2-E_{\vec{k}}\right)\end{pmatrix}\times\begin{pmatrix}\cos\zeta_{\vec{k}}\\ -\sin\zeta_{\vec{k}}\end{pmatrix}=0, \tag{3.18}$$

where $E_{\vec{k}}$ is the energy of a state and $\cos\zeta_{\vec{k}}$ and $\sin\zeta_{\vec{k}}$ are the coefficients of the corresponding wave function. The energy below the gap is given by

$$E_{\vec{k}}=\frac{\hbar^2}{2m}(k^2+\tfrac{1}{4}Q^2)^2-\frac{1}{2}\left[\left(\frac{\hbar^2}{m}(\vec{k}\cdot\vec{Q})\right)^2+G^2\right]^{1/2}. \tag{3.19}$$

Above the gap, the energy is given by Eq. (3.19), with a plus sign between the two terms. In calculating the resistivity, the electron scatters between states near the Fermi surface, and this, in the present case, includes states only below the gap. We may write Eq. (3.19) in a simpler form if we assume that $\vec{Q}$ is along the k_z axis and if we define the following dimensionless units,

$$\kappa=(k_x^2+k_y^2)^{1/2}/Q,\quad w=k_z/Q,\quad \alpha=mG/\hbar^2Q^2. \tag{3.20}$$

With these definitions, Eq. (3.19) becomes

$$E_{\vec{k}}=\frac{\hbar^2Q^2}{2m}[(\kappa^2+w^2+\tfrac{1}{4})-(w^2+\alpha^2)^{1/2}]. \tag{3.21}$$

The corresponding wave function is given by

$$\Psi_{\vec{k}}=\cos\zeta_{\vec{k}}e^{i[\vec{k}+(Q/2)]\cdot\vec{r}}-\sin\zeta_{\vec{k}}e^{i[\vec{k}-(Q/2)]\cdot\vec{r}}, \tag{3.22}$$

where

$$\cos\zeta_{\vec{k}} = \frac{\alpha/\sqrt{2}}{(w^2+\alpha^2)^{1/4}[w+(w^2+\alpha^2)^{1/2}]^{1/2}}, \quad (3.23)$$

and the phase is chosen for the state below the gap such that

$$\sin 2\zeta_{\vec{k}} = \frac{\alpha}{(w^2+\alpha^2)^{1/2}}. \quad (3.24)$$

Note that the system is cylindrically symmetric and that the wave-function coefficients are independent of κ. Also, for $w=0$, $\sin\zeta_{\vec{k}} = \cos\zeta_{\vec{k}} = 1/\sqrt{2}$. In Fig. 5, we plot in (a) the energy spectrum (below the gap), in (b) the corresponding wave-function coefficients, and in (c) the Fermi surface centered in our new coordinate system with its origin at the gap. For the Fermi surface, we have assumed the case of critical contact at the gap.[24] The equation for this Fermi surface is given by

$$\kappa = [(w^2+\alpha^2)^{1/2} - \alpha - w^2]^{1/2}. \quad (3.25)$$

Only in the conical regions of the Fermi surface, which result from the CDW, are the energy spectrum and wave functions severely distorted from the plane-wave state. For this reason, it is only in this region that electron-phason scattering is intense, as we will see below.

We now turn to a calculation of the matrix element of Eq. (3.16). We use the wave functions defined by Eq. (3.22) and the interaction $V_{e\phi}$ given by Eq. (3.14) to obtain

$$M_{\vec{k},\vec{k}'} = \left(\frac{G}{4}\right)\sum_{\vec{q}} \phi_{\vec{q}}[\langle\Psi_{\vec{k}'}, n_{\vec{q}}-1,\ldots|a_{\vec{q}}(e^{i(\vec{q}+\vec{Q})\cdot\vec{r}} - e^{i(\vec{q}-\vec{Q})\cdot\vec{r}})|\Psi_{\vec{k}}, n_{\vec{q}},\ldots\rangle$$
$$+\langle\Psi_{\vec{k}'}, n_{-\vec{q}}+1,\ldots|a^*_{-\vec{q}}(e^{i(\vec{q}+\vec{Q})\cdot\vec{r}} - e^{i(\vec{q}-\vec{Q})\cdot\vec{r}})|\Psi_{\vec{k}}, n_{\vec{q}},\ldots\rangle], \quad (3.26)$$

as the only nonvanishing terms. When we evaluate this expression explicitly, we may write the transition rate directly as

$$W_{\vec{k}\to\vec{k}'} = H(\vec{k},\vec{k}')f_{\vec{k}}(1-f_{\vec{k}'})[n_{\vec{q}}\delta(E_{\vec{k}}-E_{\vec{k}'}+\hbar\omega_{\vec{q}}) + (n_{-\vec{q}}+1)\delta(E_{\vec{k}}-E_{\vec{k}'}-\hbar\omega_{\vec{q}})], \quad (3.27)$$

where

$$H(\vec{k},\vec{k}') = \frac{2\pi}{\hbar}\left(\frac{G}{4}\right)^2\phi^2_{\vec{q}}C^2_{\vec{k},\vec{k}'} \quad (3.28)$$

and

$$C^2_{\vec{k},\vec{k}'} = (\cos\zeta_{\vec{k}}\sin\zeta_{\vec{k}'} - \cos\zeta_{\vec{k}'}\sin\zeta_{\vec{k}})^2, \quad (3.29)$$

with $\vec{q}=\vec{k}'-\vec{k}$. Note that $H(\vec{k},\vec{k}')$ is symmetric with respect to interchange of $\vec{k}$ and $\vec{k}'$.

In writing Eqs. (3.27)–(3.29), we have neglected the scattering just at the center of the belly of the Fermi surface. For the geometry we have chosen in Fig. 5, these belly-to-belly transitions would be considered "umklapp" scattering, while the conical-point-to-conical-point transitions would be considered normal transitions. However, in a conventional geometry (centered at the left-hand edge of Fig. 5), these belly-to-belly transitions would be seen to be no different than transitions within each belly, which are negligible in magnitude compared with the scattering within the conical-point regions.

In fact, the overwhelming contribution to the electron-phason scattering is concentrated in the conical-point regions of the Fermi surface. This can be seen most easily by an examination of Fig. 5, with the help of Eq. (3.29). The wave-function coefficients enter the scattering rate in the form $\cos\zeta_{\vec{k}'}\sin\zeta_{\vec{k}}$. From Figs. 5(b) and 5(c), it is clear that $\cos\zeta_{\vec{k}}$ and $\sin\zeta_{\vec{k}}$ are both appreciable only in the conical-point regions of the Fermi surface.

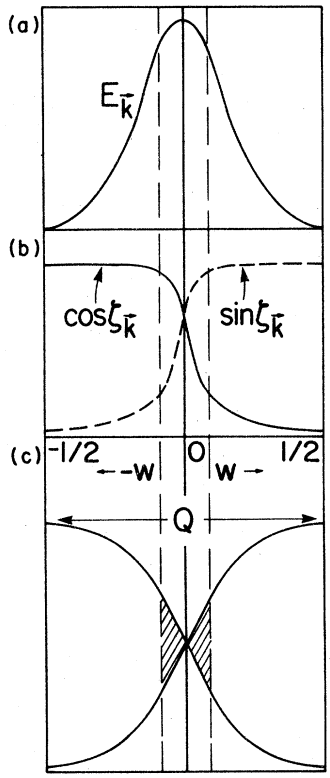

FIG. 5. (a) Electron energy band $E_{\vec{k}}$ [Eq. (3.21)], (b) coefficients of the wave function $\cos\zeta_{\vec{k}}$ and $\sin\zeta_{\vec{k}}$ [Eqs. (3.22–(3.24)], and (c) Fermi surface for a CDW system with the origin at the CDW gap.

Since phasons are confined to a very small region of $\vec{k}$ space, as is indicated in Figs. 3 and 4, $\vec{q}=\vec{k}'-\vec{k}$ is always small. Therefore, $\vec{k}$ is nearly the same as $\vec{k}'$, and $\cos\zeta_{\vec{k}'}\sin\zeta_{\vec{k}}$ is large in the same regions as $\cos\zeta_{\vec{k}}\sin\zeta_{\vec{k}}$, which is in the conical-point regions. This can also be seen from Eqs. (3.23) and (3.24). For this reason, it is possible to neglect belly scattering compared with conical-point scattering.

Since the only appreciable scattering is in the conical-point regions of the Fermi surface, we can simplify the problem at hand by assuming that the Fermi surface consists of two intersecting cones, which can be obtained from Eq. (3.25) by assuming that $|w|\ll 1$. The new Fermi surface is then written as

$$\kappa\simeq\beta|w|, \tag{3.30}$$

where

$$\beta=\left(\frac{1}{2\alpha}-1\right)^{1/2}. \tag{3.31}$$

Similarly, we approximate the velocities of the electron to be consistent with this new Fermi surface,

$$v_z\simeq-\left(\frac{\hbar Q}{m}\right)\beta^2 w, \tag{3.32}$$

$$v_x\simeq\left(\frac{\hbar Q}{m}\right)\kappa\cos\theta, \tag{3.33}$$

with κ given by Eq. (3.30) and θ the polar angle of cylindrical coordinates. Since the system is cylindrically symmetric, we need only consider the x and z components of velocity.

In Sec. IV, we will employ the transition rate in Eq. (3.27) in order to derive expressions for the resistivity. In doing so, we will employ the simplified Fermi surface of two intersecting cones.

IV. DERIVATION OF THE ELECTRON-PHASON RESISTIVITY

The residual resistivity in potassium in the temperature region of interest here is at least 3 orders of magnitude larger than the temperature-dependent resistivity. That is, the scattering of electrons from impurities and other imperfections in the crystal dominates over the scattering of any temperature-dependent mechanism. For this reason, this scattering will determine the shape of the steady-state electron distribution function. Therefore, we will make the same assumption that we made in a calculation of the residual resistivity for a CDW model of K,[24] namely, that the steady-state electron distribution function (relevant for electron-phason scattering) is that of the rigidly shifted equilibrium distribution function. We then balance the total momentum of the electrons arising from an external electric field with the total momentum due to collisions of electrons with phasons. This is equivalent to a variational solution of the Boltzmann transport equation. A detailed discussion of this method is given in Ref. 24, where it was used in the calculation of the residual resistivity anisotropy in potassium assuming the electrons to be in a CDW ground state.

The rigidly shifted electron distribution function is given by[40]

$$f(\vec{k})=f_0(\vec{k}-\vec{\delta})\approx f^0_{\vec{k}}-\hbar\delta_\mu v_{\vec{k}\mu}\frac{\partial f^0_{\vec{k}}}{\partial E_{\vec{k}}}, \tag{4.1}$$

where $f^0_{\vec{k}}$ is the equilibrium distribution and the electric field $\vec{\mathcal{E}}$ is assumed to be in the μ direction such that

$$\delta_\mu=-e\mathcal{E}_\mu\tau_\mu/\hbar, \tag{4.2}$$

where $v_{\vec{k}\mu}=(1/\hbar)\partial E_{\vec{k}}/\partial k_\mu$ is the μ component of the velocity of an electron in the state $|\Psi_{\vec{k}}\rangle$. In the absence of collisions, electrons under the influence of $\vec{\mathcal{E}}$ would be accelerated such that $f^0_{\vec{k}}$ would translate at a constant rate in $\vec{k}$ space. Then τ_μ would simply be the length of time after $f^0_{\vec{k}}$ was centered at $\vec{k}=0$. When collisions are included, δ_μ is independent of time once the system has reached a steady state, and τ_μ is the relaxation time.

We begin the derivation of the electron phason resistivity[41] with the Boltzmann transport equation, which equates the rate of change of the electron distribution function $f_{\vec{k}}$ due to the electric field $\vec{\mathcal{E}}$ with that due to collisions,

$$-e(\vec{v}_{\vec{k}}\cdot\vec{\mathcal{E}})\frac{\partial f^0_{\vec{k}}}{\partial E_{\vec{k}}}=\int\frac{d^3k'}{8\pi^3}(W_{\vec{k}'\to\vec{k}}-W_{\vec{k}\to\vec{k}'}), \tag{4.3}$$

where $W_{\vec{k}\to\vec{k}'}$, given by Eq. (3.27) of Sec. III, is the transition rate for electrons leaving the state $\vec{k}$ by scattering to the state $\vec{k}'$, and $W_{\vec{k}'\to\vec{k}}$ is the rate for electrons entering the state $\vec{k}$ from $\vec{k}'$.

We can transform Eq. (4.3) into the equation for the balance of the total momentum of the electrons by multiplying both sides of the equation by $v_{k\nu}$ and integrating over d^3k. Then, if the electric field is in the μ direction, the left-hand side of the equation vanishes unless $\mu=\nu$. Thus,

$$L_\mu\mathcal{E}_\mu=-\hbar\delta_\mu I_\mu, \tag{4.4}$$

where

$$L_\mu=-e\int\frac{d^3k}{4\pi^3}v^2_{\vec{k}\mu}\frac{\partial f^0_{\vec{k}}}{\partial E_{\vec{k}}}, \tag{4.5}$$

and

$$I_\mu = \frac{-1}{\hbar\delta_\mu}\int\frac{d^3k}{4\pi^3}\int\frac{d^3k'}{8\pi^3}(W_{\vec{k}'\to\vec{k}} - W_{\vec{k}\to\vec{k}'}). \tag{4.6}$$

L_μ can be evaluated explicitly, yielding,

$$L_x = L_y = ne/m, \tag{4.7a}$$

$$L_z = neF/m, \tag{4.7b}$$

where n is the electron density, with

$$F = 3\left(\frac{m}{\hbar Q}\right)^2\left(\frac{Q}{k_F}\right)^3\int_0^{1/2} v_{\vec{k}z}^2\, dw, \tag{4.8}$$

where we have used the variables $E_{\vec{k}}$, w, and θ of Sec. III in Eqs. (3.20), (3.21), and (3.33) together with the transformation

$$d^3k = \left(\frac{m}{\hbar^2}\right)Q\, d\theta\, dw\, dE_{\vec{k}} \tag{4.9}$$

to evaluate L_z.

The μ component of the current density in the metal is given by

$$J_\mu = -e\int\frac{d^3k}{4\pi^3}\vec{v}_{\vec{k}\mu}f_{\vec{k}} = -\hbar\delta_\mu L_\mu = \frac{L_\mu^2}{I_\mu}\mathcal{E}_\mu. \tag{4.10}$$

The resistivity tensor is diagonal in this coordinate system and is given formally by

$$\rho_{\mu\mu} = \frac{I_\mu}{L_\mu^2} = \frac{m}{ne^2\tau_\mu}. \tag{4.11}$$

The remaining problem is to calculate I_μ. First, we note that if we invoke the identity,

$$n_{\vec{q}}f^0_{\vec{k}}(1-f^0_{\vec{k}'}) = (n_{\vec{q}}+1)f^0_{\vec{k}'}(1-f^0_{\vec{k}}), \tag{4.12}$$

we may write the transition rates, from Eq. (3.27), more simply as

$$\begin{aligned}(W_{\vec{k}'\to\vec{k}} - W_{\vec{k}\to\vec{k}'}) = H(\vec{k},\vec{k}')\{&[f_{\vec{k}'}(1-f_{\vec{k}}) - f^0_{\vec{k}'}(1-f^0_{\vec{k}})][(n_{\vec{q}}+1)\delta(E_{\vec{k}}-E_{\vec{k}'}+\hbar\omega_{\vec{q}}) + n_{\vec{q}}\delta(E_{\vec{k}}-E_{\vec{k}'}-\hbar\omega_{\vec{q}})]\\ &-[f_{\vec{k}}(1-f_{\vec{k}'}) - f^0_{\vec{k}}(1-f^0_{\vec{k}'})][n_{\vec{q}}\delta(E_{\vec{k}}-E_{\vec{k}'}+\hbar\omega_{\vec{q}}) + (n_{\vec{q}}+1)\delta(E_{\vec{k}}-E_{\vec{k}'}-\hbar\omega_{\vec{q}})]\}.\end{aligned} \tag{4.13}$$

Then we use the relation Eq. (4.1) for the rigidly displaced electron distribution function $f_{\vec{k}}$ together with the identity

$$\frac{\partial f^0_{\vec{k}}}{\partial E_{\vec{k}}} = \frac{-f^0_{\vec{k}}(1-f^0_{\vec{k}})}{k_BT} \tag{4.14}$$

to obtain

$$(W_{\vec{k}'\to\vec{k}} - W_{\vec{k}\to\vec{k}'}) = -\frac{\hbar\delta_\mu}{k_BT}(v_{\vec{k}\mu} - v_{\vec{k}'\mu})H(\vec{k},\vec{k}')n_{\vec{q}}[f^0_{\vec{k}}(1-f^0_{\vec{k}'})\delta(E_{\vec{k}}-E_{\vec{k}'}+\hbar\omega_{\vec{q}}) - f^0_{\vec{k}'}(1-f^0_{\vec{k}})\delta(E_{\vec{k}}-E_{\vec{k}'}-\hbar\omega_{\vec{q}})]. \tag{4.15}$$

If we multiply Eq. (4.15) by $v_{\vec{k}\mu}$, integrate over d^3k and d^3k', and then interchange $\vec{k}$ and $\vec{k}'$ in the term containing $\delta(E_{\vec{k}}-E_{\vec{k}'}-\hbar\omega_{\vec{q}})$ we can write a simplified form for I_μ,

$$I_\mu = \frac{1}{k_BT}\int\frac{d^3k}{4\pi^3}\int\frac{d^3k'}{8\pi^3}H(\vec{k},\vec{k}')(v_{\vec{k}\mu} - v_{\vec{k}'\mu})^2 n_{\vec{q}}f^0_{\vec{k}}(1-f^0_{\vec{k}'})\delta(E_{\vec{k}}-E_{\vec{k}'}+\hbar\omega_{\vec{q}}). \tag{4.16}$$

Since the system has cylindrical symmetry, we transform from $\vec{k}$ and $\vec{k}'$ to the coordinates of energies $E_{\vec{k}}$, $E_{\vec{k}'}$ and the cylindrical coordinates w, w', θ, and θ' of Sec. III. In doing so, we make use of Eq. (4.9). We also write explicitly the expression for $H(\vec{k},\vec{k}')$ from Eq. (3.28) of Sec. III. The scattering integral I_μ then becomes

$$\begin{aligned}I_\mu = &\frac{\pi}{(8\pi^3)^2}\left(\frac{mQ}{\hbar^2}\right)^2\left(\frac{G}{A}\right)^2\left(\frac{1}{\rho_m k_B T}\right)\\ &\times\int dw\int dw'\int d\theta\int d\theta'\int dE_{\vec{k}}\int dE_{\vec{k}'}(v_{\vec{k}\mu} - v_{\vec{k}'\mu})^2 C^2_{\vec{k},\vec{k}'}\left(\frac{n_{\vec{q}}}{\omega_{\vec{q}}}\right)f^0_{\vec{k}}(1-f^0_{\vec{k}'})\delta(E_{\vec{k}}-E_{\vec{k}'}+\hbar\omega_{\vec{q}}),\end{aligned} \tag{4.17}$$

where, as in Eqs. (3.27)–(3.29), $\vec{q} = \vec{k}' - \vec{k}$. $f^0_{\vec{k}}\times(1-f^0_{\vec{k}'})$ is nearly a delta function of energy at the Fermi surface. By comparison, the quantities $(v_{\vec{k}\mu} - v_{\vec{k}'\mu})^2$ and $C^2_{\vec{k},\vec{k}'}$ are slowly varying in energy in this region, so that it is reasonable to replace them by their values at the Fermi surface in the evaluation of the integrals over energy. With this assumption, the energy-dependent part of I_μ is

$$\begin{aligned}U &= \int dE_{\vec{k}}\int dE_{\vec{k}'}\, f^0_{\vec{k}}(1-f^0_{\vec{k}'})\delta(E_{\vec{k}}-E_{\vec{k}'}+\hbar\omega_{\vec{q}})\\ &= \int dE_{\vec{k}}\, f_0(E_{\vec{k}})[1-f_0(E_{\vec{k}}+\hbar\omega_{\vec{q}})].\end{aligned} \tag{4.18}$$

With the definitions,

$$f_0(E_{\vec{k}}) = \frac{1}{(e^{\eta}+1)}, \quad \eta = \frac{(E_{\vec{k}} - E_F)}{k_B T} \tag{4.19}$$

$$n_{\vec{q}} = \frac{1}{(e^{z}-1)}, \quad z = \frac{\hbar\omega_{\vec{q}}}{k_B T} \tag{4.20}$$

U may be evaluated as

$$U = (k_B T)\int_{-E_F/k_B T}^{\infty} d\eta \frac{e^{\eta+z}}{(e^{\eta}+1)(e^{\eta+z}+1)} \cong \frac{(k_B T)z}{(1-e^{-z})} \tag{4.21}$$

and

$$\left(\frac{n_{\vec{q}}}{\omega_{\vec{q}}}\right) U = \left(\frac{\hbar e^{-z}}{(1-e^{-z})^2}\right). \tag{4.22}$$

In obtaining Eq. (4.21), we have used the fact that since $(E_F/k_B T)$ is large and at the lower limit of the integral the integrand is nearly zero, the integral is essentially unchanged if we replace the lower limit by $-\infty$.

In the angular integrations of Eq. (4.17), over θ and θ', we first transform to the new angles $\psi = \theta - \theta'$ and $\psi' = \frac{1}{2}(\theta + \theta')$, so that $d\theta d\theta' = d\psi d\psi'$. Then the only factor that depends on ψ' is $(v_{\vec{k}\mu} - v_{\vec{k}'\mu})^2$. If we define

$$(\bar{v}_\mu - \bar{v}'_\mu)^2 = \left(\frac{m}{\hbar Q}\right)^2 \left(\frac{1}{2\pi}\right) \int_{-\pi}^{\pi} d\psi' (v_{\vec{k}\mu} - v_{\vec{k}'\mu})^2, \tag{4.23}$$

then, with the help of Eqs. (3.32) and (3.33), where the approximate forms of $v_{\vec{k}\mu}$ are given, we may write

$$(\bar{v}_x - \bar{v}'_x)^2 = \tfrac{1}{2}(\kappa^2 + \kappa'^2) - \kappa\kappa' \cos\psi, \tag{4.24a}$$

$$(\bar{v}_z - \bar{v}'_z)^2 = \beta^4 (w - w')^2. \tag{4.24b}$$

At this point, since the integrand is even in the variables ψ and w, we agree to integrate only over the positive part of the integration regions of both variables and to multiply the result by 4. (That is, we integrate over the allowed part of ψ between 0 and π and over the allowed part of w between 0 and $\frac{1}{2}$.)

Next we make a change of variables to center of mass and relative coordinates,

$$\tilde{\xi} = \tfrac{1}{2}(w + w'), \tag{4.25}$$

$$\tilde{q}_z = q_z/Q = w - w', \tag{4.26}$$

so that $d\tilde{\xi} d\tilde{q}_z = dw dw'$. We then change from the variable $\tilde{q}_z$ to z, which was defined in Eq. (4.20). The relation between $\tilde{q}_z$ and z is

$$\tilde{q}_z^2 = \frac{4\left[\left(\frac{T}{\Theta_\phi}\right)^2 \left(\frac{q_\phi}{2Q}\right)^2 z^2 - \frac{\eta^2\beta^2}{2}\tilde{\xi}^2(1-\cos\psi)\right]}{1 + \frac{\eta^2\beta^2}{2}(1+\cos\psi)}, \tag{4.27}$$

$$dw dw' = d\tilde{\xi} d\tilde{q}_z = \frac{d\tilde{\xi}(z\,dz)}{\tilde{q}_z}\left(\frac{T}{\Theta_\phi}\right)^2 \left(\frac{q_\phi}{2Q}\right)^2 \frac{1}{[1 + \frac{1}{2}\eta^2\beta^2(1+\cos\psi)]}, \tag{4.28}$$

where the phason temperature $\Theta_\phi = \hbar\omega_\phi/k_B T$, with $\omega_\phi = c_{\|} q_\phi$, and the wave-vector cutoff q_ϕ of the phason spectrum in the k_z direction were defined in Eq. (3.5) and indicated in Figs. 3 and 4. With the assumption of this frequency cutoff for the phason spectrum, the range of integration for z is from 0 to (Θ_ϕ/T).

The other limits of integration are found simply if we assume the model of two intersecting cones described at the end of Sec. III and defined in Eq. (3.30). The maximum value $\tilde{\xi}_{\max}$ for $\tilde{\xi}$ is actually approximately the average of the maximum values of w and w', which is $\frac{1}{2}$. However, the integrand becomes negligibly small before that, so that for the purposes of numerical integration, this is set at a convenient value. In fact, it is this same localization of the electron-phason scattering near the conical points that allows us to use such a simple approximation for the Fermi surface.

In order to determine the lower limit on $\tilde{\xi}$, we recall that we agreed to integrate only over $w \geq 0$. The integration is then divided into two regions, $w \geq 0$, $w' \geq 0$, or $\tilde{\xi}^2 \geq \frac{1}{4}\tilde{q}_z^2$, or scattering of electrons within a single conical point, and $w \geq 0$, $w' \leq 0$, or $\tilde{\xi}^2 \leq \frac{1}{4}\tilde{q}_z^2$, or scattering of electrons from conical point to conical point. The condition $\tilde{\xi}^2 = \frac{1}{4}\tilde{q}_z^2$ then enables us to determine the lower limit on $\tilde{\xi}$, so that

$$-z\left(\frac{T}{\Theta_\phi}\right)\left(\frac{q_\phi}{2Q}\right)\Big/(1+\eta^2\beta^2)^{1/2} \leq \tilde{\xi} \leq \tilde{\xi}_{\max}, \tag{4.29}$$

where we ensure that $w \geq 0$ by choosing $\tilde{q}_z \geq 0$. The two regions $w \geq 0$, $w' \leq 0$ and $w \geq 0$, $w' \geq 0$ are separated by $z(T/\Theta_\phi)(q_\phi/2Q)/(1+\eta^2\beta^2)^{1/2}$. For $\tilde{\xi}$ greater than this value, the scattering is within a single conical region.

The maximum value $\psi_{\max}$ for ψ is determined by requiring that $\tilde{q}_z^2 \geq 0$. Also, $\psi_{\max}$ is never greater than π. The integration is then divided most simply into two regions. The first is

$$-z\left(\frac{T}{\Theta_\phi}\right)\left(\frac{q_\phi}{2Q}\right)\Big/(1+\eta^2\beta^2)^{1/2} \leq \tilde{\xi} \leq \frac{z}{\eta\beta}\left(\frac{T}{\Theta_\phi}\right)\left(\frac{q_\phi}{2Q}\right), \quad 0 \leq \psi \leq \pi, \tag{4.30}$$

and the second is

$$\frac{z}{\eta\beta}\left(\frac{T}{\Theta_\phi}\right)\left(\frac{q_\phi}{2Q}\right) \leq \tilde{\xi} \leq \tilde{\xi}_{\max},$$

$$0 \leq \psi \leq \cos^{-1}\left[1 - \left(\frac{2z^2}{\eta^2\beta^2\tilde{\xi}^2}\right)\left(\frac{T}{\Theta_\phi}\right)^2\left(\frac{q_\phi}{2Q}\right)^2\right]. \tag{4.31}$$

A further approximation that we will make concerns the part of the square of the scattering matrix element $C^2_{\vec{k},\vec{k}'}$, that is defined in Eq. (3.29). The cutoff q_ϕ of $\vec{q}$ in the z direction is only about 10^{-3} of the distance from the conical point to the belly of the Fermi surface, so that $\tilde{q}_z$ is always a small quantity. For this reason, we write $C^2_{\vec{k},\vec{k}'}$ in terms of $\tilde{\xi}$ and $\tilde{q}_z$, and expand in powers of $\tilde{q}_z$, keeping only the lowest-order term. Then $C^2_{\vec{k},\vec{k}'}$ becomes

$$C^2_{\vec{k},\vec{k}'} \cong \left(\frac{\tilde{q}_z^2}{4\alpha^2}\right)\hat{C}^2(\tilde{\xi}), \tag{4.32}$$

where

$$\hat{C}^2(\tilde{\xi}) = \frac{\alpha^4}{(\tilde{\xi}^2+\alpha^2)^2}. \tag{4.33}$$

Combining all these integrations, approximations, and transformations of variables, we can finally write Eq. (4.6) in the form

$$I_\mu = \hat{I}_\mu/\bar{\tau}, \tag{4.34}$$

where

$$\frac{1}{\bar{\tau}} = \left(\frac{Q^4}{8\pi^4}\right)\left(\frac{m}{n\rho_m}\right)\left(\frac{G}{A}\right)^2\left(\frac{1}{\hbar k_B \Theta_\phi}\right), \tag{4.35}$$

and

$$\hat{I}_\mu = \left(\frac{1}{\alpha^2}\right)\left(\frac{q_\phi}{2Q}\right)^2\left(\frac{T}{\Theta_\phi}\right) \times \int_0^{\Theta_\phi/T} dz\left(\frac{ze^{-z}}{(1-e^{-z})^2}\right)\int_{\tilde{\xi}_{\min}}^{\tilde{\xi}_{\max}} d\tilde{\xi}\,\hat{C}^2(\tilde{\xi}) \int_0^{\psi_{\max}} S_\mu(z,\tilde{\xi},\psi)\frac{\left[\left(\frac{T}{\Theta_\phi}\right)^2\left(\frac{q_\phi}{2Q}\right)^2 z^2 - \frac{1}{2}\eta^2\beta^2\tilde{\xi}^2(1-\cos\psi)\right]^{1/2}}{[1+\frac{1}{2}\eta^2\beta^2(1+\cos\psi)]^{5/2}}, \tag{4.36}$$

where

$$S_z(z,\tilde{\xi},\psi) = 8\beta^4\left[\left(\frac{T}{\Theta_\phi}\right)^2\left(\frac{q_\phi}{2Q}\right)^2 z^2 - \tfrac{1}{2}\eta^2\beta^2\tilde{\xi}^2(1-\cos\psi)\right], \tag{4.37a}$$

$$S_x(z,\tilde{\xi},\psi) = 2\beta^2\left[\left(\frac{T}{\Theta_\phi}\right)^2\left(\frac{q_\phi}{2Q}\right)^2 z^2(1+\cos\psi) + \tilde{\xi}^2(1-\cos\psi)\right], \tag{4.37b}$$

where the endpoints $\tilde{\xi}_{\min}, \tilde{\xi}_{\max}, \psi_{\max}$, are determined by Eqs. (4.30) and (4.31).

The components of the temperature-dependent resistivity tensor due to electron-phason scattering may now be written, from Eqs. (4.6), (4.11) and (4.34), as

$$\rho_{xx} = \rho_{yy} = \left(\frac{m}{ne^2\bar{\tau}}\right)\hat{I}_x, \tag{4.38a}$$

$$\rho_{zz} = \left(\frac{m}{ne^2\bar{\tau}}\right)\frac{\hat{I}_z}{F^2}. \tag{4.38b}$$

$\hat{I}_x$ and $\hat{I}_z$ of Eqs. (4.36) and (4.37) must be obtained in general by three-dimensional numerical integration, which will be discussed in Sec. V.

The calculation of the contribution to the low-temperature resistivity can be understood in terms of a very simple picture. When one derives the Bloch-Grüneisen formula for the electron-phonon resistivity one assumes that the phonon spectrum is isotropic and that the Fermi surface is spherical. One than pictures the center of a phonon sphere moving along the surface of the Fermi sphere. The position of the center of this phonon sphere marks the initial state $\vec{k}$ of an electron and any point within the phonon sphere, but on the Fermi surface, is an allowed scattered state $\vec{k}'$ of the electron. For very low temperatures, as the temperature decreases, the effective size of the phonon sphere decreases, giving rise to a T^5 dependence in the low-temperature limit. For electron-phason scattering, we have an analogous situation, which is shown in Fig. 6. The phason spectrum is anisotropic, and we assume a fre-

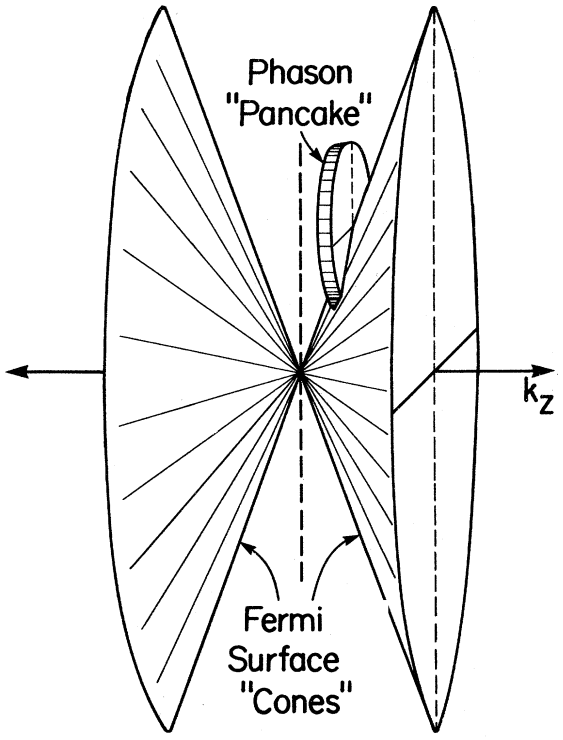

FIG. 6. Phason "pancake" riding along the surface of the Fermi-surface "cones."

quency cutoff, so that the phonon sphere, for the case of the Bloch-Grüneisen formula, becomes here a phason "pancake," an ellipsoid of revolution, where the ratio of the width to the diameter of the "pancake" is the anisotropy parameter η, defined in Eq. (3.4). Since we have assumed the Fermi surface to be two intersecting cones, we can now picture, as in Fig. 6, the center of the phason "pancake" riding along the surface of the Fermi-surface "cones." An electron in the state $\vec{k}$ at the center of the phason "pancake" may scatter to any state $\vec{k}'$ on the Fermi surface that is within the phason "pancake." As in the case of phonons, for very low temperatures the phason "pancake" decreases in size, leading again to a T^5 dependence in the low-temperature limit, as long as the anisotropy parameter is not too small.

In order to understand what happens in the case of an extremely anisotropic phason spectrum, let us consider the limit of infinite anisotropy, i.e., $\eta \to 0$. In this case, the integrals reduce simply to Bloch-Grüneisen functions, $\mathcal{G}_n(x)$, as was pointed out in Ref. 8. If we keep Θ_ϕ and q_ϕ finite as $\eta \to 0$, then $\hat{I}_x$ and $\hat{I}_z$ become

$$\hat{I}_x = \left(\frac{2\pi\beta^2}{\alpha^2}\right)\left[A_1\left(\frac{q_\phi}{2Q}\right)^3\left(\frac{T}{\Theta_\phi}\right)^2 \mathcal{G}_2\left(\frac{\Theta_\phi}{T}\right) + A_2\left(\frac{q_\phi}{2Q}\right)^5\left(\frac{T}{\Theta_\phi}\right)^4 \mathcal{G}_4\left(\frac{\Theta_\phi}{T}\right) + \left(\frac{q_\phi}{2Q}\right)^6\left(\frac{T}{\Theta_\phi}\right)^5 \mathcal{G}_5\left(\frac{\Theta_\phi}{T}\right)\right], \tag{4.39a}$$

$$\hat{I}_z = \left(\frac{8\pi\beta^4}{\alpha^2}\right)\left[A_2\left(\frac{q_\phi}{2Q}\right)^5\left(\frac{T}{\Theta_\phi}\right)^4 \mathcal{G}_4\left(\frac{\Theta_\phi}{T}\right) + \left(\frac{q_\phi}{2Q}\right)^6\left(\frac{T}{\Theta_\phi}\right)^5 \mathcal{G}_5\left(\frac{\Theta_\phi}{T}\right)\right], \tag{4.39b}$$

with

$$A_1 = \int_0^{\tilde{\xi}_{\max}} d\tilde{\xi}\left(\frac{\alpha^4\tilde{\xi}^2}{(\tilde{\xi}^2+\alpha^2)^2}\right), \quad A_2 = \int_0^{\tilde{\xi}_{\max}} d\tilde{\xi}\left(\frac{\alpha^4}{(\tilde{\xi}^2+\alpha^2)^2}\right), \tag{4.40}$$

plus small terms of order $(q_\phi/2Q)^7(T/\Theta_\phi)^6\mathcal{G}_6(\Theta_\phi/T)$. The Bloch-Grüneisen functions are defined as

$$\mathcal{G}_n(x) = \int_0^x \frac{e^{-z}dz}{(1-e^{-z})^2}. \tag{4.41}$$

The factor of $\sqrt{2}$ that appeared in Ref. 8 in the $\mathcal{G}_5$ term was incorrect.

We note that, in this limiting case, the low-temperature limiting dependence is no longer T^5. In fact, the $\mathcal{G}_2$ term varies as T^2 and the $\mathcal{G}_4$ term as T^4. This is due to the fact that, in the limit $\eta \to 0$, the diameter of the phason "pancake" becomes infinite so that the allowed scattering is from an initial state located on the Fermi surface at w (along the z direction) to a point w' that is located within the region on the Fermi surface between $w \pm q_\phi$. Thus, there is no restriction in the x and y directions. This means that, as the temperature decreases, the effective volume of the phason "pancake" that encloses the Fermi surface does not decrease as rapidly as if the "pancake" were not so anisotropic.

In Sec. V, we will present the results of numerical integration of $\hat{I}_\mu$ in Eq. (4.36) with $\eta \neq 0$. In addition, we will show that comparing the magnitude of the resistivity predicted by this theory with that of existing data enables us to determine an allowed range for the anisotropy parameter η.

V. NUMERICAL RESULTS

In this section, we will present the results of the numerical evaluations of the three-dimensional integrals $\hat{I}_x$ and $\hat{I}_z$ in Eqs. (4.36) and (4.37) in the form of the components of the electron-phason resistivity tensor given by Eq. (4.38). Since these numerical computations presented considerable difficulties, it is worthwhile to discuss briefly the procedure used to calculate the integrals. The integral over ψ caused no difficulty. However, in the integral over $\tilde{\xi}$, the integrand varies rapidly in parts of the integration region and must be handled carefully. We used a Gauss-Legendre iterative scheme that divides the regions more finely where the function is rapidly varying and more coarsely where it is slowly varying. Also, in the integration region of Eq. (4.31), we employed the transformation

$$x = \tilde{\xi}/(a+\tilde{\xi}), \tag{5.1}$$

and used x as the integration variable. If equal intervals are chosen for x, then intervals for $\tilde{\xi}$ will be close together for small $\tilde{\xi}$ and far apart for large $\tilde{\xi}$. This is useful, since the function decays in this region as $\tilde{\xi}$ increases. a is chosen to optimize the procedure. In the integration over z, we use the same type of transformation as for $\tilde{\xi}$ in Eq. (5.1), since the largest part of the integrand is located where z is small. If one tries to perform the integrations over $\tilde{\xi}$ and z with a uniform grid of points, a much larger amount of computer time is needed than with the procedures described here.

The magnitude of the calculated electron-phason resistivity agrees very well with the range of experimentally observed values, for reasonable values of the parameters in the theory. In addition, the resistivity tensor due to electron-phason scattering is highly anisotropic, which can explain the sample dependence of the data. The resistivity ρ_{zz} along $\vec{Q}$ is much larger than the re-

sistivity ρ_{xx} or ρ_{yy} perpendicular to $\vec{Q}$. Since there are 24 equally preferred directions for $\vec{Q}$ in K,[30] one would expect that most samples would not consist of a single domain, i.e., $\vec{Q}$ pointing in the same direction throughout the sample. Rather, many $\vec{Q}$ domains would exist. The domain structure would vary from sample to sample and from run to run on the same sample, depending, perhaps in some uncontrolled way, on the experimental procedures. The effects of these $\vec{Q}$ domains on the residual resistivity were discussed in Ref. 24. Since the residual resistivity is anisotropic by a factor of 4 or 5 to 1, the residual resistivity can change by as much as this factor, with no change in the number of impurities or other imperfections in the sample. Similarly, since the electron-phason resistivity is highly anisotropic, this part of the resistivity can also change if the domain structure changes. In addition, the magnitude of the electron phason resistivity will be correlated with the residual resistivity in such a way as to produce an apparent breakdown of Matthiessen's rule. In fact, Matthiessen's rule need not be violated in order to explain the data. That is, one can add the contributions from the residual resistivity and from the electron-phason resistivity independently and still find a correlation between the residual resisitivity and the temperature-dependent electron-phason resistivity, as is observed in experiments.

The parameters in Eqs. (4.35)–(4.37) that we adjust in order to fit the data are the phason temperature Θ_ϕ, which determines the shape of the resistivity curve, and the anisotropy parameter η, which determines the magnitude of the temperature-dependent part of the data. In order to take into account the $\vec{Q}$-domain structure, we write the total resistivity $\rho(T)$ in the temperature range of the data points in Fig. 1 below 1.3 K as,

$$\rho(T)=\rho_0+x\rho_{zz}+(1-x)\rho_{xx}\,, \tag{5.2}$$

where x is between 0 and 1 and where the electron-phason resistivities ρ_{zz} and ρ_{xx} are given by Eq. (4.38). This means that a fraction x of the domains are along $\vec{Q}$ and a fraction $(1-x)$ are perpendicular to $\vec{Q}$. The procedure is to determine a value of Θ_ϕ [Eq. (3.5)] that fits the shape of the data, and for a given value of η [Eq. (3.4)], determine x for a particular sample. The result of such a procedure, with $\Theta_\phi = 3.25$ K, is the smooth curve through the data in Fig. 1, or the horizontal line ρ (phason) in Fig. 2. We recall that, in Fig. 1, the resistivity was set at 0 for the lowest data point, for experimental convenience, so that the residual resistivity should actually be added to all the data points.

In Fig. 7, we plot the magnitudes of the components of the electron-phason resistivity tensor, ρ_{xx} and ρ_{zz}, as a function of the anisotropy of the phason spectrum $(1/\eta)$. As can be seen from the figure, the resistivity increases rapidly with increasing isotropy. For the phason temperature, we have used the value $\Theta_\phi = 3.25$ K, which produced the fit to the data in Fig. 1. The other values of constants used in the calculations displayed in Fig. 7 are as follows. We employ the average transverse-phason velocity, which was calculated by Giuliani and Overhauser[26] to be $c_\perp = 1.40\times 10^5$ cm/sec, where $c_\perp$ is defined in Eq. (3.4a). The phason wave-vector cutoff q_ϕ along $\vec{Q}$ is given, from Eq. (3.5), by

$$q_\phi = k_B\Theta_\phi\eta/c_\perp\,. \tag{5.3}$$

We choose a value for the CDW gap energy $G/E_F^0 = 0.35$ that is within the range determined by previous experiments,[24] where the Fermi energy in the absence of a CDW is $E_F^0 = 2.12$ eV. For the CDW wave vector $\vec{Q}$, we choose a magnitude consistent with Ref. 24, so that for this value of G, $Q/k_F = 2.149$, where $E_F^0 = \hbar^2k_F^2/2m$. The dimensionless constant $\alpha = 0.0379$ is obtained from Eq. (3.20), and then β is given by Eq. (3.31). The

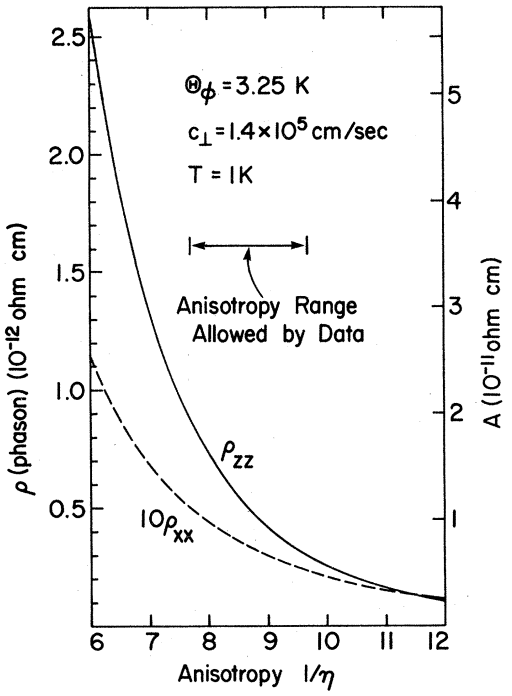

FIG. 7. Plot of the electron phason resistivities ρ_{xx} and ρ_{zz} [Eq. (4.38)] as a function of anisotropy $(1/\eta)$. The range of anisotropies consistent with the data of Refs. 1–4 is shown by the double-headed arrow. On the right-hand vertical scale, A is the coefficient of the Bloch-Grüneisen function $(T/\Theta_\varphi)^5\mathcal{J}_5(\Theta_\varphi/T)$ that fits the calculated values of the electron-phason resistivity.

maximum amplitude A [Eq. (3.7)] of the ions from their equilibrium positions has been calculated by Giuliani and Overhauser[30] to be $A \cong 0.03$ Å. The electron density is $n = 1.402 \times 10^{22}$ cm^{-3}, and the mass density is $\rho_m = 0.910$.

An examination of Fig. 7, together with the magnitudes of the temperature-dependent part of the resistivity found in experiments,[1-4] permits us to identify a range of values of the anisotropy $1/\eta$ that are consistent with the data. For simplicity, we compare all values for $T = 1$ K. While not all sets of data included this temperature, this is the simplest way of comparing the measurements, since Refs. 1 and 3 quote their results in terms of the coefficient a of aT^2 that was used in an attempt to fit the temperature-dependent part of the data. For the data that did not include $T = 1$ K, we simply use the value of that coefficient as the extrapolated value. This gives essentially $\rho - \rho_0$, where ρ_0 is guessed to fit the data. Although this is admittedly a crude procedure, it gives a reasonable idea of the range of magnitudes of the resistivity. This range extends from about 0.05 to 0.29 nΩ cm at $T = 1$ K.

If we assume that the largest value observed, $\rho - \rho_0 \cong 0.29$ nΩ cm, corresponded to all the $\vec{Q}$ domains in the sample lying parallel to the length of the wire, i.e., $x = 1$, then we obtain the maximum possible value of the anisotropy, $1/\eta = 9.7$, that fits the data. For the smallest value observed, $\rho - \rho_0 \cong 0.05$ nΩ cm, we suppose that all the domains were perpendicular to the length of the wire, i.e., $x = 0$. Then we obtain the smallest anisotropy, $1/\eta = 7.7$, that is consistent with the data. The actual anisotropy probably lies somewhere between these two extreme values, as is indicated in Fig. 7.

An interesting result of the numerical calculations is that the shape of the resistivity curve resulting from these evaluations is very nearly the same shape as the Bloch-Grüneisen function $\mathcal{G}_5(\Theta/T)$ of Eq. (4.41), multiplied by T^5. This is exactly the same function that appears in the simple Bloch-Grüneisen formula for electron-phonon scattering. The shapes of ρ_{xx} and ρ_{zz} agree with $(T/\Theta_\phi)^5 \mathcal{G}_5(\Theta_\phi/T)$ to within 1% in the region of the data in Fig. 1, although the extrapolation at zero temperature is slightly lower for this calculation. The $\mathcal{G}_5$ function extrapolates to −11.5 on the vertical scale of Fig. 1, while the true function extrapolates to −12.0. For the purposes of analyzing the data, therefore, it might be useful to use the relation

$$\rho(T) \cong \rho_0 + [xA_z + (1-x)A_x](T/\Theta_\phi)^5 \mathcal{G}_5(\Theta_\phi/T) \quad (5.4)$$

in order to determine parameters of this theory consistent with the data, where the values of A_x and A_z for a given anisotropy can be read from the right-hand vertical scale of Fig. 7, for $\Theta_\phi = 3.25$ K. This procedure could save considerable computation time. A_z is determined from our calculation by setting $x = 1$, while A_x is determined by setting $x = 0$.

Although we have determined an allowable range of values of the anisotropy that are consistent with the data, as shown in Fig. 7, there is some flexibility in that range. For instance, we have chosen an average value of the transverse-phason velocity. Giuliani and Overhauser[26] found that the transverse-phason spectrum is actually quite anisotropic, with velocities along the two principal transverse directions given by $c_2 = 2.08 \times 10^5$ cm/sec and $c_3 = 0.94 \times 10^5$ cm/sec, where the value we have used in Fig. 7 is the geometric mean, $c_\perp = 1.40 \times 10^5$ cm/sec. Assuming that some other average for $c_\perp$ might be more appropriate, we plot in Fig. 8 the magnitudes of ρ_{xx} and ρ_{zz} as a function of $c_\perp$ that ranges between these two extreme values. We see that both ρ_{xx} and ρ_{zz} increase rapidly with decreasing $c_\perp$. A smaller value of $c_\perp$ would thus move the allowed range of anisotropies in Fig. 7 to higher values of $(1/\eta)$. Again, we have labeled the right-hand vertical scale with the magnitude of the coefficient A of the Bloch-Grüneisen function, as in Eq. (5.4).

Another factor in the magnitude of the resistivity is the phason temperature Θ_ϕ. Both ρ_{xx} and ρ_{zz} increase rapidly with increasing Θ_ϕ. The depen-

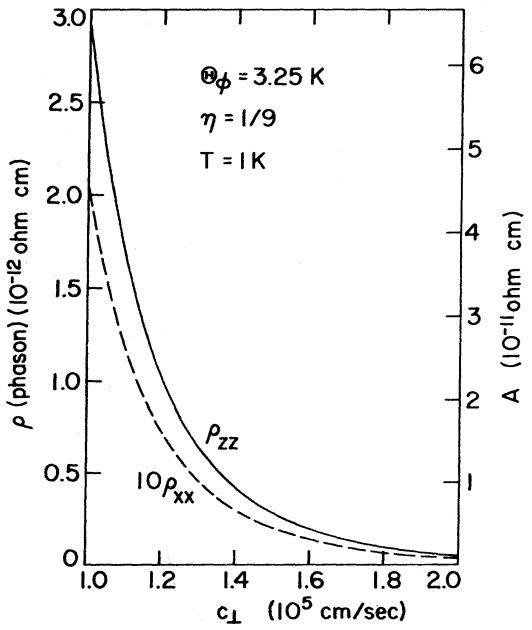

FIG. 8. Plot of the electron-phason resistivities ρ_{xx} and ρ_{zz} as a function of the transverse-phason velocity $c_\perp$. A has the same meaning as in Fig. 7.

dences of the electron-phason resistivity on the parameters Θ_ϕ, $c_\perp$, and η can be understood qualitatively by considering the effects of each of these parameters on the total phase space occupied by the phasons. This can be seen by examining Fig. 4. Since increasing Θ_ϕ is the same as increasing ω_ϕ, the frequency cutoff, this enlarges the phase space occupied by phasons and therefore increases the resistivity. As $c_\perp$ decreases, the volume of the anisotropic cone of the phason spectrum increases, so that the resistivity increases. If the phason spectrum becomes more isotropic while $c_\perp$ is kept fixed, this is the same as decreasing the longitudinal phason velocity $c_\parallel$, so that the phase space increases and so does the resistivity.

VI. CONCLUSIONS

We have found that the theory of electron-phason scattering can explain the shape, the magnitude, as well as the sample dependence of the anomalous temperature-dependent resistivity in potassium below 1.3 K. In addition, we have ruled out all other explanations that have been proposed to explain the data. A comparison of our theory with the data determines parameters of phasons that enter the theory. The phason temperature that gives the best fit to the data is $\Theta_\phi = 3.25$ K, and the approximate range of acceptable values of the anisotropy of the phason spectrum is $7.7 \lesssim (1/\eta) \lesssim 9.7$. This is the same order of magnitude as the anisotropy in rubidium, $(1/\eta) \approx 11$, which was determined by attributing to phasons the anomaly in the specific heat of Rb.[36] Another feature is that we find the shape of the resistivity curve to be almost the same as that of the famous Bloch-Grüneisen formula for the temperature-dependent resistivity due to normal electron-phonon scattering. Of course, that formula uses instead the phonon Debye temperature $\Theta_D \sim 90$ K.

In this calculation, we have assumed that the CDW in K produces only one gap, which is located at $\pm\vec{Q}$, at the conical points of the Fermi surface. (See Fig. 5.) However, many orientations of open orbits have been observed in K,[29] suggesting that other gaps, resulting from the multiple periodicity of the lattice and the CDW are also important. Electron-phason scattering would probably be intense near each of these gaps on the Fermi surface and could increase the resistivity above what is calculated here. That would have the result of translating the range of allowed anisotropies to higher values of $(1/\eta)$.

It would be useful to have further sensitive measurements on high-purity samples of the temperature-dependent resistivity of K. Measurements should be done that extend from 1.3 K to the lowest possible temperatures in order to test the theory presented here. However, since the electron-phason resistivity should decrease very rapidly below the temperature range of existing data, with a low-temperature limit of T^5, it is likely that the contribution of electron-electron scattering, with its T^2 temperature dependence, would appear before the electron-phason T^5 dependence is actually achieved. In fact, electron-electron scattering should be enhanced in the presence of a CDW by umklapp scattering from conical point to conical point on the Fermi surface. This would make the electron-electron scattering anisotropic, depending on the direction of the CDW wave vector $\vec{Q}$ with respect to the electric field. Then, if the $\vec{Q}$-domain structure changed from sample to sample, the electron-electron scattering would also be sample dependent.

ACKNOWLEDGMENTS

The authors would like to thank J. A. Rowlands for providing the data shown in Figs. 1 and 2 and for many useful discussions. In addition, the authors are grateful to the National Science Foundation and the NSF Materials Research Laboratory Program for support of this research.

[1] H. van Kempen, J. S. Lass, J. H. J. M. Ribot, and P. Wyder, Phys. Rev. Lett. 37, 1574 (1976).
[2] J. A. Rowlands, C. Duvvury, and S. B. Woods, Phys. Rev. Lett. 40, 1201 (1978), and private communication.
[3] B. Levy, M. Sinvani, and A. J. Greenfield, Phys. Rev. Lett. 43, 1822 (1979).
[4] J. H. J. M. Ribot, Doctoral Dissertation, Katholieke Universiteit te Nijmegen, 1979 (unpublished).
[5] H. van Kempen, J. H. J. M. Ribot, and P. Wyder, J. Phys. (Paris) 39, C6 1048 (1978); J. H. J. M. Ribot, J. Bass, H. van Kempen, and P. Wyder, J. Phys. F 9, L117 (1979).
[6] M. Khoshnevisan, W. P. Pratt, P. A. Schroeder, S. Steenwyk, and C. Uher, J. Phys. F 9, L1 (1979).
[7] M. Koshnevisan, W. P. Pratt, Jr., P. A. Schroeder, and S. D. Steenwyk, Phys. Rev. B 19, 3873 (1979).
[8] Marilyn F. Bishop and A. W. Overhauser, Phys. Rev. Lett. 42, 1776 (1979).
[9] A. W. Overhauser, Phys. Rev. B 3, 3173 (1971).
[10] J. M. Ziman, *Electrons and Phonons* (Oxford University Press, London, 1960).
[11] D. Gugan, Proc. R. Soc. London A325, 223 (1971); J. W. Ekin and B. W. Maxfield, Phys. Rev. B 4, 4215 (1971).
[12] M. Kaveh and N. Wiser, Phys. Rev. B 9, 4042 (1974); 9, 4053 (1974); Phys. Rev. Lett. 29, 1374 (1972).

[13]C. R. Leavens and M. J. Laubitz, Solid State Commun. 15, 1909 (1974); J. Phys. F 5, 1519 (1975); R. Taylor, C. R. Leavens and R. C. Shukla, Solid State Commun. 19, 809 (1976); R. C. Shukla and Roger Taylor, J. Phys. F 6, 531 (1976).
[14]Klaus Fröböse, Z. Phys. B 26, 19 (1977).
[15]W. E. Lawrence and J. W. Wilkins, Phys. Rev. B 7, 2317 (1973); Carl A. Kukkonen and Henrik Smith, *ibid.* 8, 4601 (1973).
[16]M. Kaveh, C. R. Leavens, and N. Wiser, J. Phys. F 9, 71 (1979).
[17]M. Kaveh and N. Wiser, J. Phys. F 10, L37 (1980).
[18]R. A. Brown, J. Phys. F 7, 1283 (1977).
[19]Z. S. Basinski, J. S. Dugdale, and A. Howie, Philos. Mag. 8, 1989 (1963).
[20]Z. S. Basinski, J. S. Dugdale, and D. Gugan, Philos. Mag. 4, 880 (1959).
[21]G. Stetter, W. Adlhart, G. Fritsch, E. Steichele, and E. Lüscher, J. Phys. F 8, 2075 (1978).
[22]B. K. Jones, Phys. Rev. 179, 637 (1969).
[23]F. W. Holroyd and W. R. Datars, Can. J. Phys. 53, 2517 (1975).
[24]Marilyn F. Bishop and A. W. Overhauser, Phys. Rev. Lett. 39, 632 (1977); Phys. Rev. B 18, 2447 (1978).
[25]A. W. Overhauser, Phys. Rev. 128, 1437 (1962); 167, 691 (1968).
[26]G. F. Giuliani and A. W. Overhauser, Phys. Rev. B 21, 5577 (1980).
[27]A. W. Overhauser, Adv. Phys. 27, 343 (1978).
[28]Z. Altounian, C. Verge and W. R. Datars, J. Phys. F 8, 75 (1978).
[29]P. G. Coulter and W. R. Datars, Phys. Rev. Lett. 45, 1021 (1980).
[30]G. F. Giuliani and A. W. Overhauser, Phys. Rev. B 20, 1328 (1979).
[31]S. A. Werner, J. Eckert, and G. Shirane, Phys. Rev. B 21, 581 (1980).
[32]G. F. Giuliani and A. W. Overhauser, Phys. Rev. B 22, 3639 (1980).
[33]M. L. Boriack and A. W. Overhauser, Phys. Rev. B 18, 6454 (1978).
[34]Anju Sawada and Takeo Satoh, J. Low Temp. Phys. 30, 455 (1978).
[35]William H. Lien and Norman E. Phillips, Phys. Rev. 133, A1370 (1964).
[36]G. F. Giuliani and A. W. Overhauser, Phys. Rev. Lett. 45, 1335 (1980).
[37]A. W. Overhauser, Hyperfine Interactions 4, 786 (1978).
[38]M. L. Boriack and A. W. Overhauser, Phys. Rev. B 17, 4549 (1978).
[39]P. A. Lee, T. M. Rice, and P. W. Anderson, Solid State Commun. 14, 703 (1974).
[40]See, for instance, J. M. Ziman, *Principles of the Theory of Solids*, 2nd ed. (Cambridge University Press, London, 1972), Chap. 7.
[41]For a similar derivation of the electron-phonon resistivity, see R. Kubo and T. Nagamiya, *Solid State Physics* (McGraw-Hill, New York, 1969), pp. 139–155.